

Phosphorus and Oxygen Dual-doped Graphene as Superior Anode Materials for Room-temperature Potassium-ion Batteries

Guangyao Ma,^a Kangsheng Huang,^a Jia-Sai Ma,^b Zhicheng Ju,^{a,*} Zheng Xing,^{a,*} Quan-chao

Zhuang,^a

^aLithium-ion Batteries Laboratory, School of Materials Science and Engineering, China University of Mining and Technology, Xuzhou 221116, P. R. China

^bSchool of Information and Technology, Shandong Women's University, Jinan, 250300, China.

Contents:

Fig. S1 XRD pattern of r-GO.

Fig. S2 TEM image of r-GO.

Fig. S3 a) XPS survey spectrum of r-GO; b) High resolution C1s XPS spectra; c) High resolution O1s spectra; d) High resolution N 1s XPS spectra.

Fig. S4 (a) TEM image of PODG, Corresponding elemental mapping images of (b) C (c) P (d) O

Fig. S5 The rate performance of r-GO.

Fig. S6 EIS spectra of the rGO electrode at the potential of 0.01 V at the 1st, 3rd, 5th, 7th and 10th cycle.

Table S1 Parameters of EIS equivalent circuit of r-GO electrode at the potential of 0.01 V at the 1st, 3rd, 5th, 7th and 10th cycle.

Table S2 Parameters of EIS equivalent circuit of PODG electrode at the potential of 0.01 V at the 1st, 3rd, 5th, 7th and 10th cycle.

Table S3 The Warburg coefficient which equals to the slope of the line $Z_{im} \sim \omega^{-1/2}$ ($\omega = 2\pi f$) in the low-frequency region at the potential of 0.01 V at the 1st, 3rd, 5th, 7th and 10th cycle.

*Corresponding author: Tel.: +86 51683591877
E-mail address: juzc@cumt.edu.cn (Z. Ju); xzh086@cumt.edu.cn

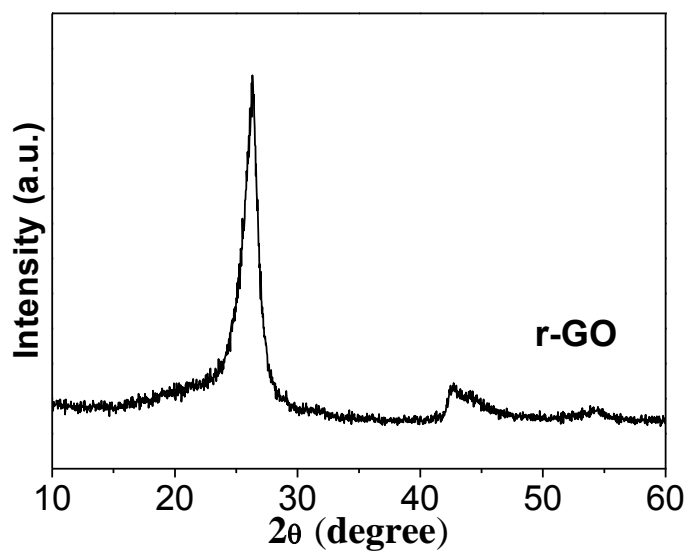


Fig. S1 XRD pattern of r-GO.

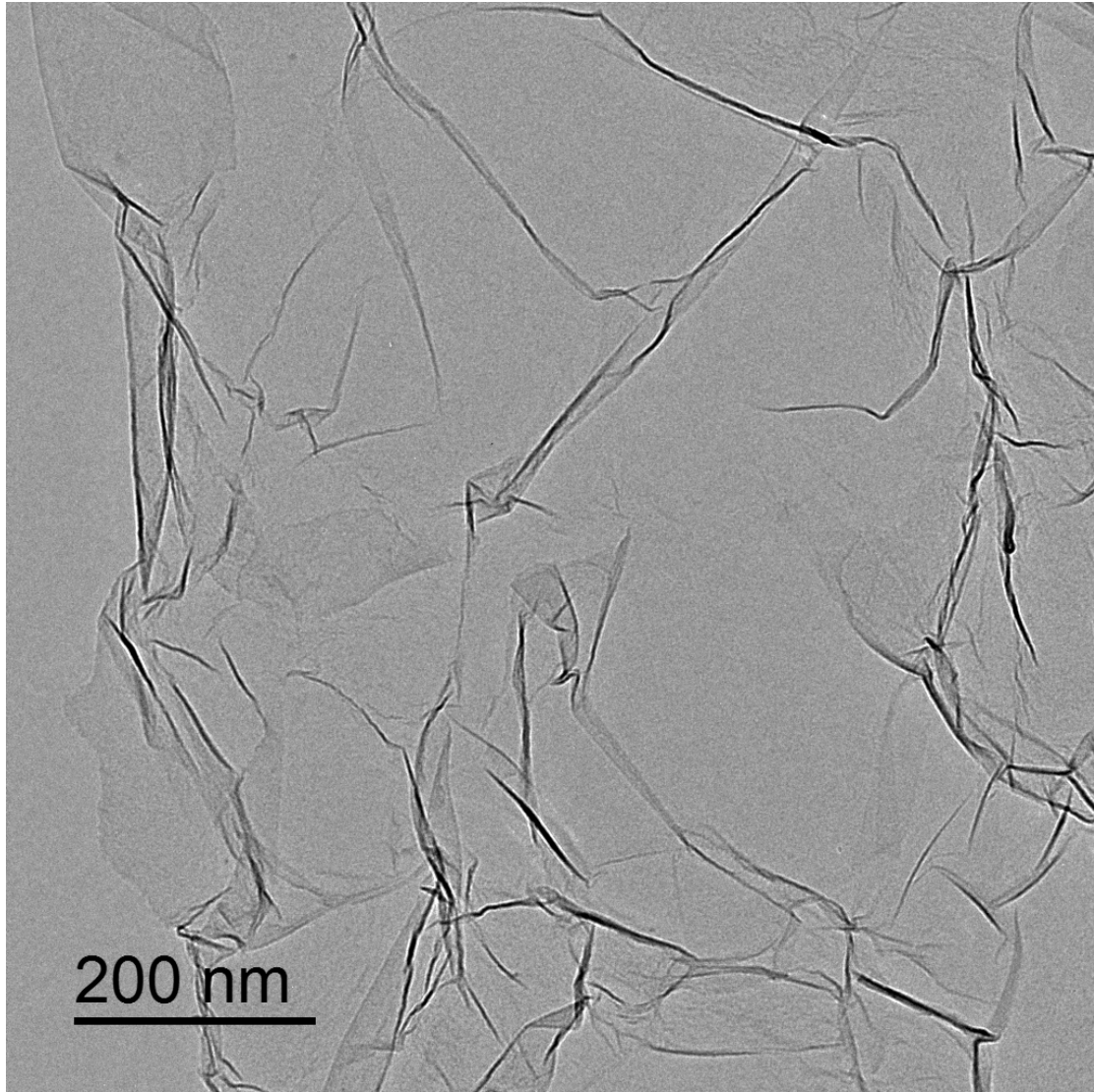


Fig. S2 TEM image of r-GO.

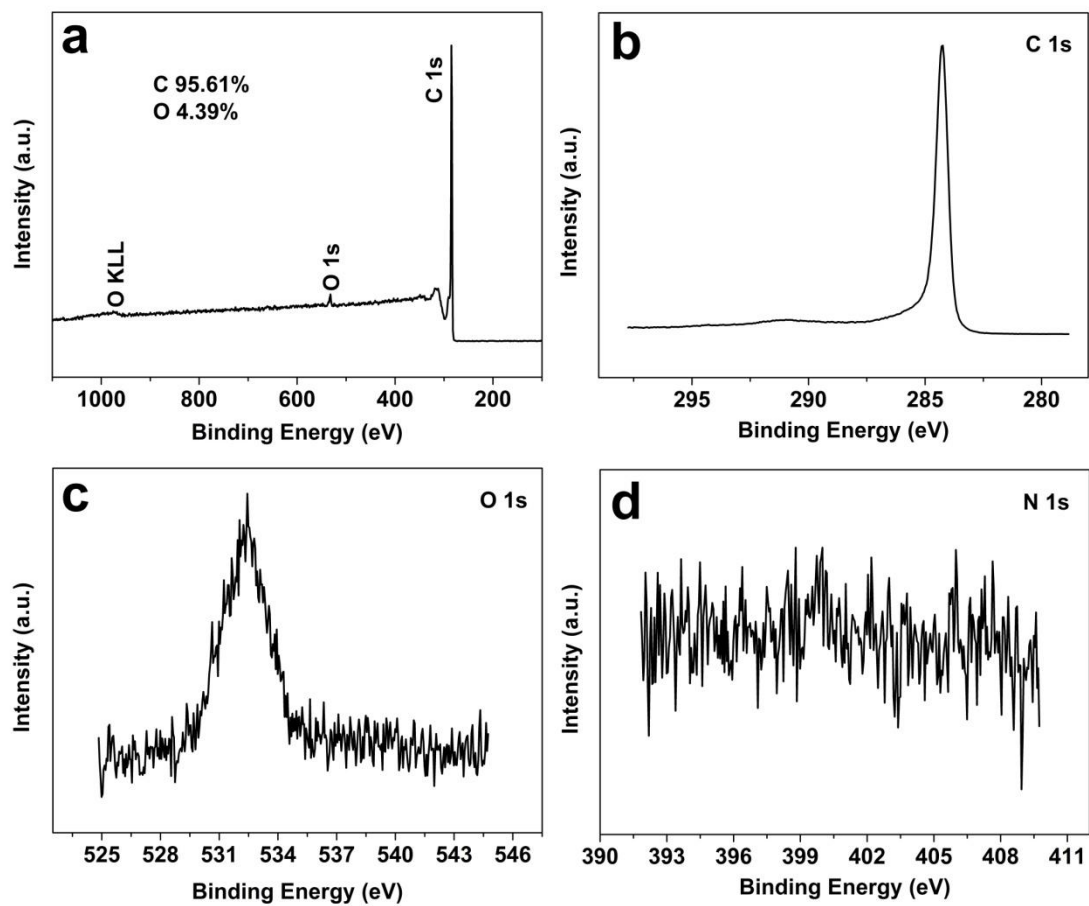


Fig. S3 a) XPS survey spectrum of r-GO; b) High resolution C1s XPS spectra; c) High resolution O1s spectra; d) High resolution N 1s XPS spectra.

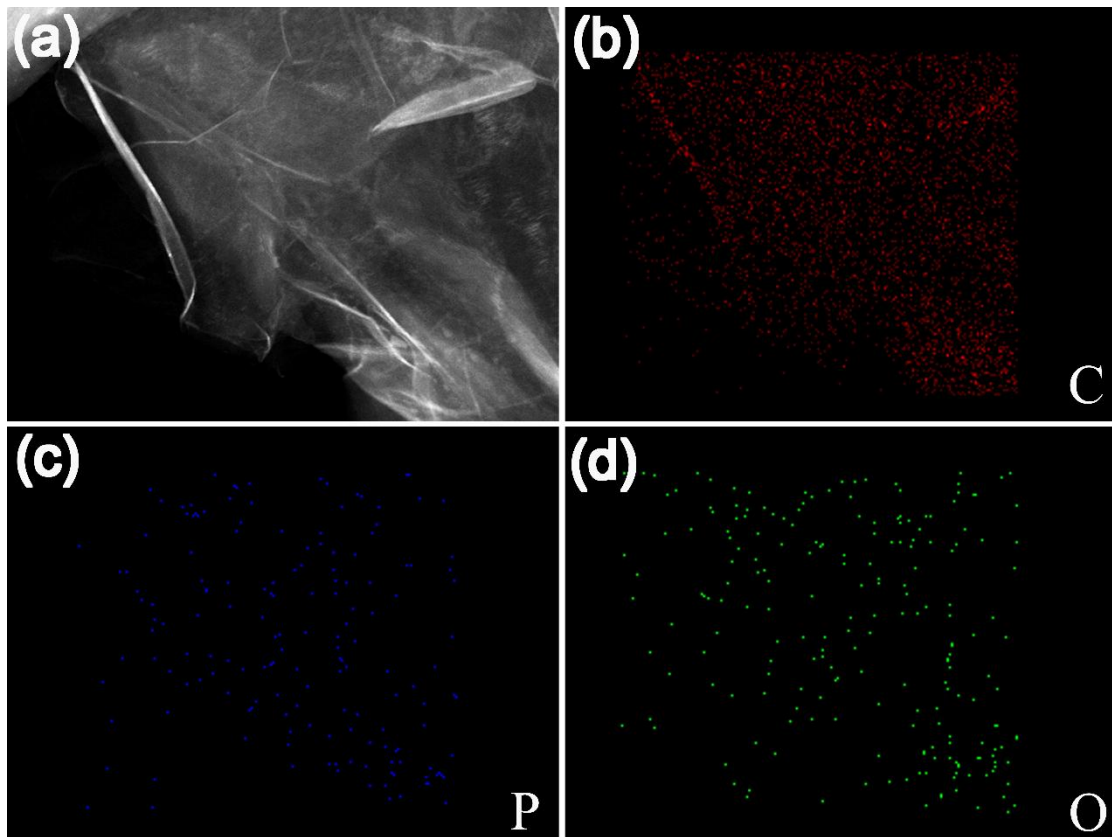


Fig. S4 (a) TEM image of PODG, Corresponding elemental mapping images of (b) C (c) P (d) O

The existence and distribution of P in the PODG was observed by element mappings of the TEM images (**Fig. S3**). The overlay of the C, P and O signals indicates that P atoms were uniformly distributed on the PODG sheets. Hence, the P and O atoms were readily incorporated into the hierarchical architectures without any significant structural destruction.

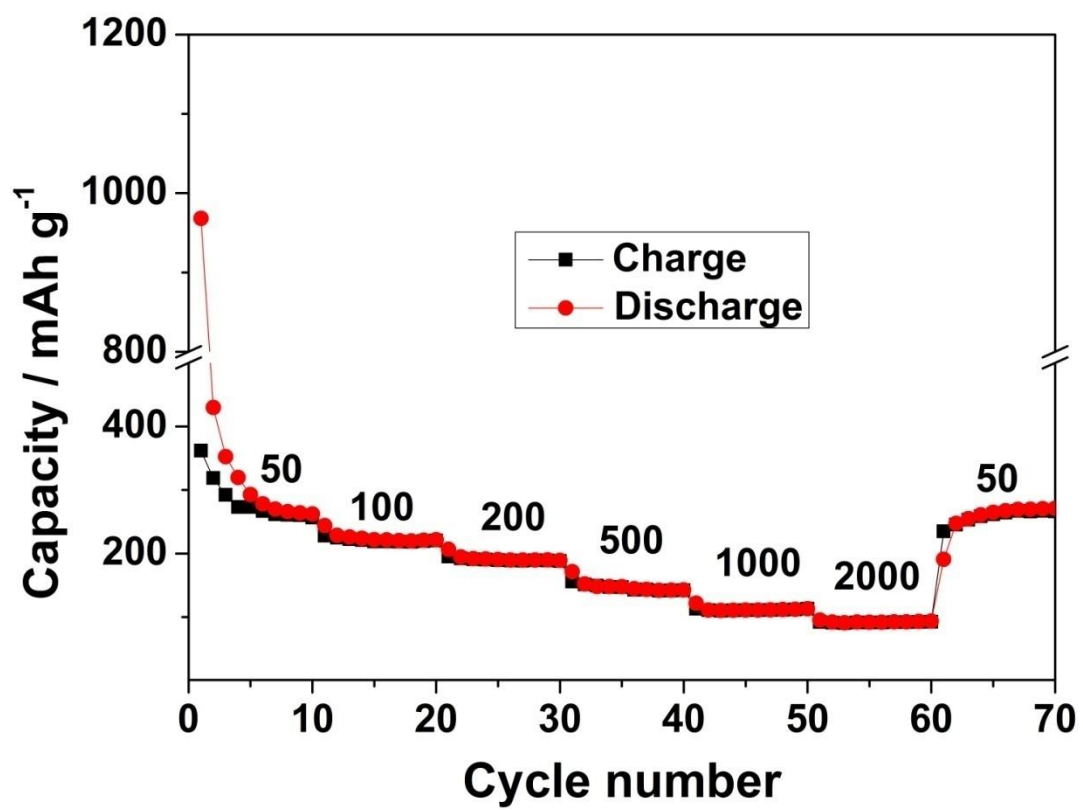


Fig. S5 The rate performance of r-GO.

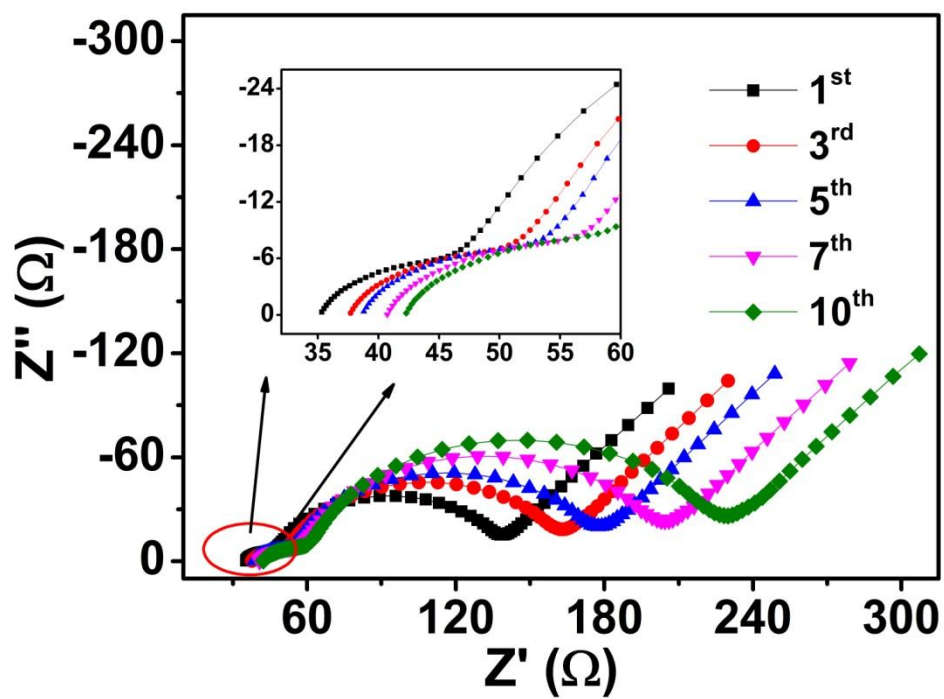


Fig. S6 EIS spectra of the rGO electrode at the potential of 0.01 V at the 1st, 3rd, 5th, 7th and 10th cycle.

In order to prove the electric conductivity of PODG is much higher than undoped graphene we take the Electrochemical Impedance Spectroscopy (EIS) of these two kinds of materials. **Fig. S6** and **Fig. 6a** shows the EIS spectra of the r-GO and PODG electrode at the potential of 0.01 V at the 1st, 3rd, 5th, 7th and 10th cycle. **Fig. 6c** shows the equivalent circuit for the EIS. The R_s , R_{SEI} , R_{ct} , and W_s represents the electrolyte resistance, the surface film resistance, the charge transfer resistance, and the Warburg resistance, respectively. **Table S1** and **Table S2** shows the parameters of EIS equivalent circuit of r-GO and PODG. The σ_e , σ_i and σ_{tol} represents the ionic conductivity, electric conductivity and total resistance of material. According to the thickness ($L=20$ um) and cross-sectional area of the electrode ($S=1.2$ cm²), the conductivity of the sample is calculated on the basis of following formula:

$$\sigma = \frac{L}{RS}$$

It's obvious that the electric conductivity of PODG is higher than undoped graphene.

Table S1 Parameters of EIS equivalent circuit of r-GO electrode at the potential of 0.01 V at the 1st, 3rd, 5th, 7th and 10th cycle

	R_s/Ω	R_{SEI}/Ω	R_{ct}/Ω	$\sigma_e/(\times 10^{-3}$ S m ⁻¹)	W_s/Ω	$\sigma_i/(\times 10^{-3}$ S m ⁻¹)	R_{tol}/Ω	$\sigma_{tol}/(\times 10^{-3}$ S m ⁻¹)
1 st	12.91	12.91	82.49	1.539	239.9	0.695	348.21	0.479
3 rd	37.54	15.6	100.7	1.083	277.3	0.601	431.14	0.387
5 th	38.59	16.78	112.1	0.995	268.9	0.619	436.37	0.382
7 th	40.66	18.28	133.6	0.866	279.4	0.597	471.94	0.353
10 th	42.15	19.67	154.3	0.771	289.3	0.576	505.42	0.329

Table S2 Parameters of EIS equivalent circuit of PODG electrode at the potential of 0.01 V at the1st, 3rd, 5th, 7th and 10th cycle

	R_s/Ω	R_{SEI}/Ω	R_{ct}/Ω	$\sigma_e/(\times 10^{-3} \text{ S m}^{-1})$	W_s/Ω	$\sigma_i/(\times 10^{-3} \text{ S m}^{-1})$	R_{tol}/Ω	$\sigma_{tol}/(\times 10^{-3} \text{ S m}^{-1})$
1 st	55.09	14.05	64.88	1.244	192.3	0.867	326.32	0.510
3 rd	55.18	15.11	86.4	1.064	204.5	0.815	361.19	0.461
5 th	56.84	16.19	125.1	0.841	218.5	0.763	416.63	0.400
7 th	53.79	16.69	131.3	0.826	212.4	0.785	414.18	0.402
10 th	52.59	16.97	143.3	0.783	226.3	0.736	439.16	0.379

Table S3 The Warburg coefficient which equals to the slope of the line $Z_{im} \sim \omega^{-1/2}$ ($\omega = 2\pi f$) in the low-frequency region at the potential of 0.01 V at the 1st, 3rd, 5th, 7th and 10th cycle

	1 st cycle	3 rd cycle	5 th cycle	7 th cycle	10 th cycle
σ' -rGO	28.899	29.976	31.339	33.187	40.442
σ' -PODG	22.699	24.669	28.247	27.851	28.075
D-rGO ($10^{-10} \text{ cm}^2 \text{ s}^{-1}$)	1.148	1.067	0.976	0.871	0.586
D-PODG ($10^{-10} \text{ cm}^2 \text{ s}^{-1}$)	1.867	1.576	1.201	1.236	1.216